Seasonal and diurnal variation of the middle atmospheric thermal structure

L. Gkouvelis (leonardos.gkouvelis@nasa.gov), *NASA Postdoctoral Program, NASA Ames Research Center, Moffett Field, CA, USA,* **A. S. Brecht**, *NASA Ames Research Center, Moffett Field, CA, USA,* **R. J. Wilson, C. E. Harman, M. A. Kahre** *NASA Ames Research Center, Moffett Field, CA, USA,* **T. Bertrand,** *LESIA, Paris Observatory, France.* **A. Kling,** *Bay Area Environmental Research Institute, Moffett Field, CA, USA.*

Introduction: The Martian middle atmosphere (~70 -140 km) climatology is greatly influenced by the lower and upper atmosphere. A variety of physical processes connects and perturbs the middle atmosphere which can feed back to other atmospheric regions (solar forcing, gravity waves, planetary waves and tides, clouds, dust storms, etc. [16], [10], [17], [18], [19], [20], [25]).

Due to observational difficulties of those atmospheric layers (too high for remote sensing observations and too low for in-situ measurements) the middle atmosphere remains the least explored region despite its importance on the overall evolution of the atmosphere. However, the observations (past and recent) that have been collected reveal the middle atmosphere to be a highly variable region. The unraveling of the complex dynamics within the middle atmosphere is key to understanding the behavior of the whole atmosphere. It has been proposed that the transport of water vapor to the upper atmosphere that leads to hydrogen escape is possible if higher temperatures prevent ice cloud formation. Dust storms can affect the temperature profile and cause stronger atmospheric circulation ([21], [22], [23]). The transport of water vapor from the lower to middle and upper atmosphere is not yet completely understood, especially to the levels that recent observations have revealed. Generally, water vapor is limited in its vertical extent by condensation. Recent discovery of a warm layer in the post-terminator at early nighttime local times have enhanced the interest in the nature and variability of this region's thermal structure ([1]). In this work we are investigating the overall thermal structure, its diurnal and seasonal variability. Through sensitivity tests with the newly extended NASA Ames Mars Climate Model (NASA Ames MGCM) we will gain physical intuition about the middle atmosphere. We utilize the most abundant retrieval observations of this region: limb and stellar occultations from the Imaging Ultraviolet Spectrograph (IUVS) instrument onboard the Mars Atmosphere and Volatile EvolutioN (MAVEN) spacecraft.

Model set up: This work will utilize the latest NASA Ames Mars Global Climate Model (MGCM), as described in [24]. The vertically extended version of the model reaches down to pressures of 10^{-6} Pa (~140-170 km depending on season and topography). Various physical schemes had to be developed and implemented in the GCM for the extended model since the main driving processes of the energy balance are the ultraviolet heating (UV), thermal conduction, and the 15 µm cooling by CO_2. These processes influence the temperature, photochemistry, and circulation of this region.
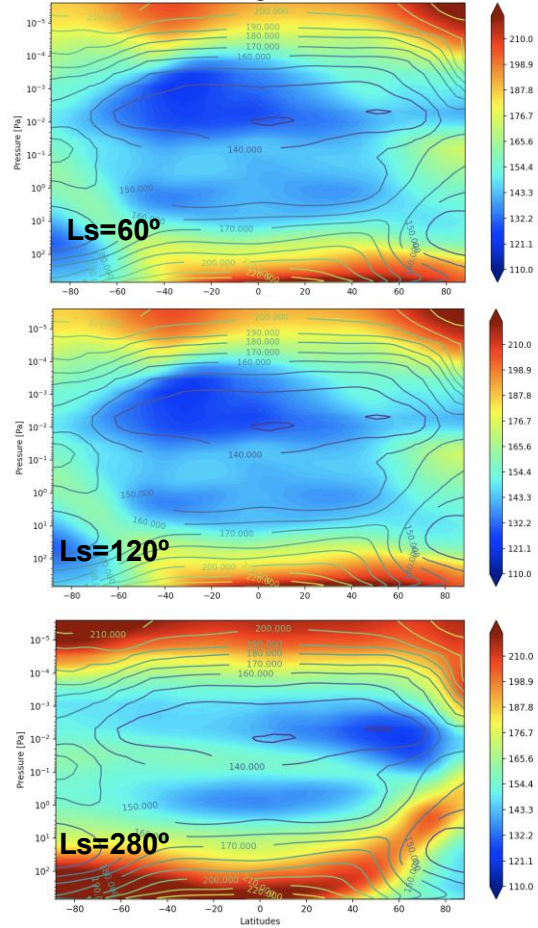

Figure 1: Zonal mean temperature field of various solar longitude positions as obtained with the GCM.

To properly account for solar UV irradiance at the top of the atmosphere we have adopted the Flare irradiance spectral model (FISM) solar spectrum model [5] which is a detailed spectrum constructed with 1-nm resolution based on observations from the Extreme Ultraviolet Monitor (EUVM) spectrograph on board MAVEN and is collecting solar energy in three bands [7]. Based on detailed simulations, we have adopted a heating efficiency of 22% [4]. The NonLTE correction to LTE is applied for altitudes higher then ~80 km for near IR heating rates and for NLTE CO_2 15 µm cooling we have adopted the scheme that is presented in [9]. Thermal conduction in the upper atmosphere of Mars is the main cooling mechanism and has been implemented in the MGCM.

The sequence of model development and more details of the physical processes currently included in the vertical extended version are described in [13],[14],[11].

Simulations and validation: In Figure 1 the zonal mean thermal structure is presented for a single simulation with minimum atmospheric dust load and medium solar activity, orographic gravity wave effects and radiatively active clouds. Preliminary comparisons with the Mars Climate Database (MCD) [3] show similar thermal structure with a difference up to ~15 K at maximum for the middle atmosphere. A first validation can be done by direct comparison with observations, such as the methodology proposed by [15],[12]. The so called "oxygen airglow isobar" is utilized for long- and short-term pressure variations of the middle atmosphere.

The "oxygen airglow isobar" consists of oxygen airglow direct observations either in the optical or ultraviolet vertical profiles where the peak intensity precisely (<1 km) indicates the pressure level of 0.39 mPa. In Figure 2 we compare 3 Martian years of MAVEN/IUVS limb profiles (Martian years 32, 33, 34) with the same isobar extracted from our single simulation. We combine three Martian years of observations (fall of 2014 to summer of 2018). The solar activity transitioned from medium to minimum during this time and regional dust storms were observed in MY32 and MY33 while MY34 had a global dust storm. The overall comparison is encouraging outside of the dust storm season and the model captures the seasonal variation of the pressure in the middle atmosphere. For solar longitudes outside 200-340°, a better agreement between data and model can be found by increasing the model CO_2 density profiles by ~20% on average. This is an indication that the model underestimates the density profile and thus the pressure level. Similar comparisons were presented for the MCD at [12], where a difference of 20% was found between the climatology datasets and IUVS observation but were overestimated on part of the MCD. Preliminary explanations of this discrepancy can be the lack of physics, limited chemistry, and a need to evaluate the current set up of the models (e.g., water cycle, dust cycle). For the solar longitudes around perihelion the various kilometers of discrepancy present a dip in the altitude variation of the isobar. This is the typical dusty season and during high atmospheric dust loading the temperature structure is affected and as a result the middle and upper atmosphere can be perturbed (i.e. [8],[2]). Furthermore, we have to note that the data are presented for MY33 and result in high peak altitudes for the isobar are collected above a regional dust storm during summer season for the southern hemisphere. More specifically, the peak present in the observations around L_s~250° resulted in a strong perturbation in the middle and upper atmosphere that previous GCM simulations could not match ([2]).
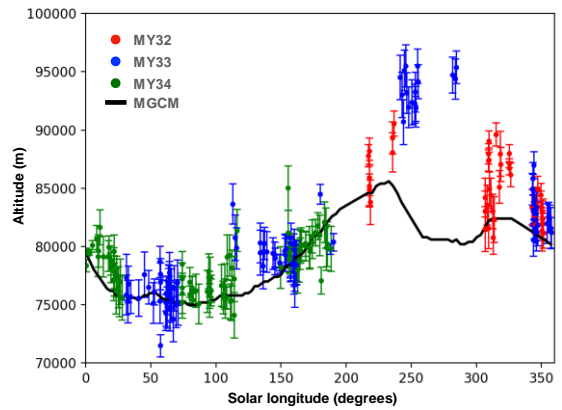

Figure 2: Observations of the oxygen airglow isobar for MY's 32, 33 and 34 from MAVEN/IUVS in limb observing mode represented by dots. Simulations for a basic scenario are shown in black solid line.

In Figure 3 the diurnal vertical thermal structure is presented for various solar longitudes. Zonal mean profiles are plotted for latitudes between -20° and 20°. We note the high variability within the middle atmosphere in comparison with altitudes lower than ~50 km and the vertical fluctuation of the mesopause around 100 to 120 km. A difference of up to 50 K is found between night and day in the middle atmosphere throughout the Martian year, while within seasons the comparison between the mean temperature is not varying more than 30 K on average. An interesting feature within our results is the appearance of a warm layer in the middle atmosphere, which is similar but weaker than the one that recently was discovered by stellar occultations limb observations from MAVEN/IUVS in the nighttime ([1]). We will look in more detail on this subject in the following section. The warm layer in our simulations is found to be at its maximum value at midnight compared to the background temperature values. It is found to be weaker but present within all local times and presents a variation in altitude, indicating vertical propagation of energy due to possible wave activity.

Comparison with retrieved temperatures: In this section we are directly comparing the simulation output with retrieved temperature profiles in the middle atmosphere. We have downloaded the MAVEN/IUVS data from the Planetary Data System (PDS) derived product level 2 which include the retrieval profiles from observations made in limb mode. The retrieval methodology is described in [1]. [1] presented results from L_s 0° to L_s 180° degrees, but in this work, we present the full database covering all IUVS stellar occultation campaigns retrieved profiles. Those cover the calendar period of early 2015 to fall of 2021. We can then have semi-continuous observations within the Martian years from 32 to 36. In Figure 4 top panel the observations are presented in altitude versus solar longitude. The observations are post terminator (SZA~110° -

130º) for both early night and a few hours before sunrise.
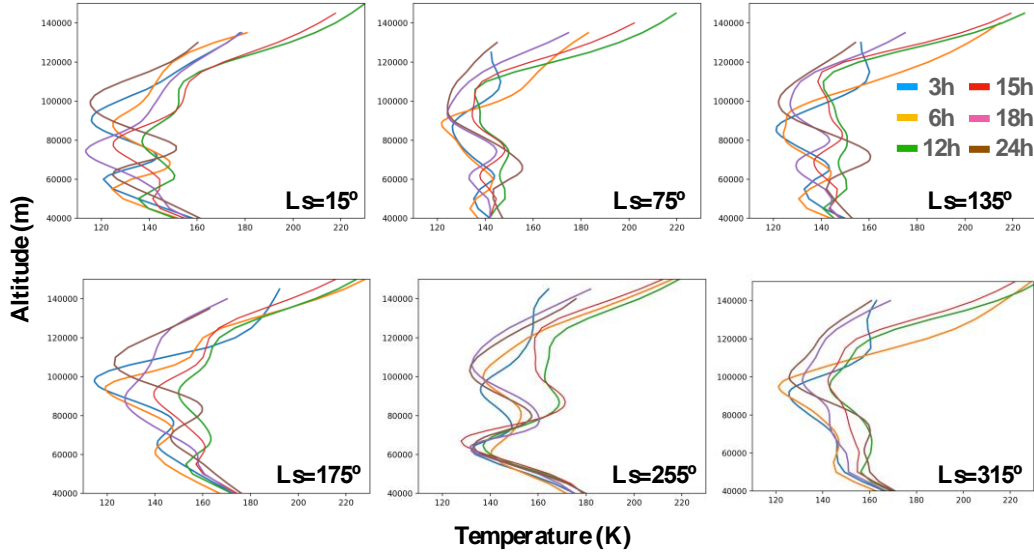

Figure 3: Equatorial (-20º -20º) latitude zonal mean profiles as obtained from the GCM.

The so-called warm layer, which was discovered in [1] for solar longitudes between 0-180º, around 80 km, it is shown here for the first time for the rest of the Martian year 180-360º degrees, since we make use of the full derived dataset. This temperature enhancement is clearly present at solar longitudes around 50º, 150º, 220º and more extended in nature around 300º which seems to be connected thermally with the lower and upper atmosphere. It presents a clear nighttime modulation across seasons with a difference of up to 40 K from the background temperature.

The mesopause can reach values down to 110 K and it seems to present an anticorrelation with the warm layer modulation, indicating that the appearance of the warm layer can have an effect in the vertical distribution upwards. In the middle panel of Figure 4 we are showing our simulations following the same sampling and plotting resolution as for the observations. The overall structure is in relatively good agreement. However, even from a visual inspection, the first difference that can be seen is the higher values the simulations present in the mesopause and a systematically warmer upper boundary. As was shown and explained in Figure 3, our simulation is producing a weaker warm layer, which is evolving diurnally with maximum intensity around midnight. Plotting our results in the same format as the observations, we can identify the warm layer in semi-continues form, and not presenting the exact same modulation. The seasonal altitude variation follows the same pattern and altitude which is an indicator that the fundamental physics behind the nature of this layer is captured by the model. As for the upper boundary, the warm layer is systematically cooler than the observations by ~20-25 K.
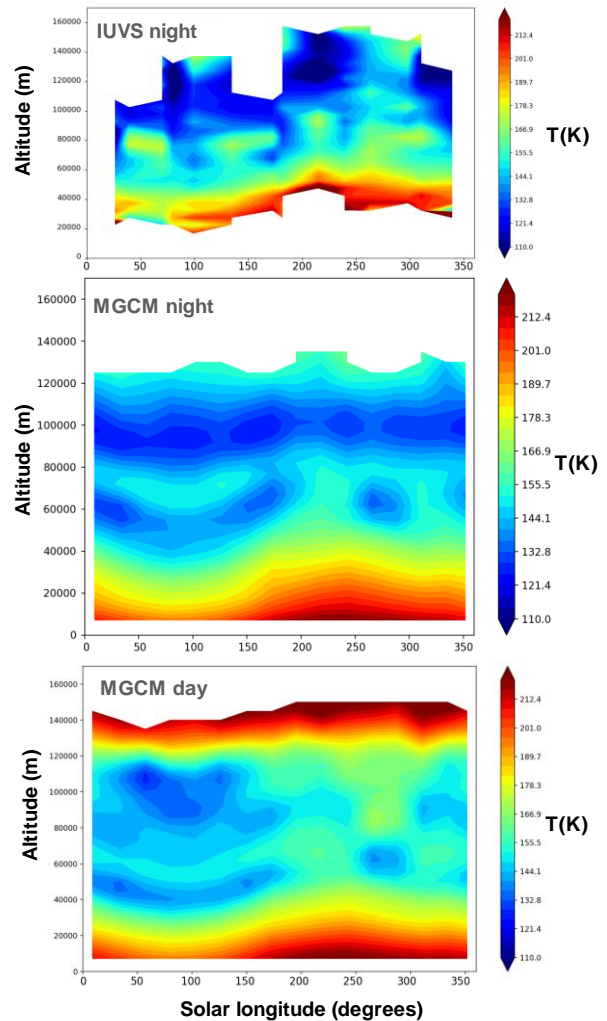

Figure 4:Top: Equatorial (-20,20) latitudes IUVS observations for nightside local times. Mid: MGCM simulation sampled identically as the observations.

Bottom: Zonal mean daytime simulation with the same resolution as the nightside.

In the bottom panel of Figure 4, zonally averaged daytime only seasonal versus altitude temperatures are presented. The warm layer appears to have a continuous shape over the year and slightly lower in altitude (compared to nighttime) of about 5-10 km.

Specific cases shown in [1] are reproduced in Figure 5, where the warm layer is found to be extremely enhanced by 30-60 K from the background level. In the same figure we overplot the simulations in black solid line for the same location and time and with colored dashed lines sequential previous and following local time steps in order to gain an evolutionary view of the thermal structure.

Discussion and prospects: This work has shown simulations combining physical mechanisms and scenarios compared with the latest and most complete observational datasets to gain physical intuition of the thermal structure and variability of the middle atmosphere. A complete catalog of simulated scenarios will be presented in the full version of this project. Our model can simulate the fundamental physics behind the thermal structure with a systematic underestimation of the temperature values, which may affect the seasonal modulation of the mesospheric warm layer. We aim to conduct a more precise comparison between model and observations, such as having the dust scenario set up for the specific MY and solar activity.

References:

[1] Nakagawa, H, et al. (2020). *Geophysical Research Letters*, *47*, e2019GL085646.
[2] Gkouvelis, L et al. (2020 *Geophysical Research Letters*, *47*(12)
[3] Millour, E., et al., 2015. EPSC abstract 2015-438, Vol. 10.
[4] Gu, H et al. (2020) *The Astronomical Journal*, *159*(2), 39.
[5] Thiemann, E. M. et al. (2017) Journal of Geophysical Research: Space Physics, 122(3), 2748-2767.
[6] Ritter, B (2019) Journal of Geophysical Research: Space Physics, 124, 4809–4832
[7] Eparvier, F. G (2015) Space Science Reviews, 195(1–4), 293–301.
[8] Withers, P., Pratt, R., 2013. Icarus 225 (1), 378–389.
[9] López- Valverde, M. A et al. (1998) *Journal of Geophysical Research: Planets*, *103*(E7),16799-16811.
[10] Bougher, S. W et al. (2014a) Cambridge Univ. Press, Cambridge, U. K.
[11] L. Gkouvelis. AGU Fall Meeting 2021, 2021
[12] Gkouvelis, L. et al. (2020) *Icarus*, *341*. 113666
[13]Brecht, A. S et al. (2014) Oxford, U.K.,
[14] Brecht, A. S et al.(2015) *European Planetary Science Congress*, Abstract, 10,EPSC2015-420.
[15] Gkouvelis, L. et. al. (2018) JGR(Planets) 123, 3119–3132.
[16] Bougher, S. W et al. (2002). *Geophys. Monogr. Ser* (Vol. 130, pp. 261–288). Washington, DC: AGU.
[17] Bougher, P.- L et al. (2008) *Space Science Reviews*, *139*(1- 4), 107–141.
[18] Bougher, S. et al. (2014) Cambridge: Cambridge University Press.
[19] Bougher, S. W et al. (2015). *JGR, Planets*, *120*, 311–342.
[20] Gonzalez- Galindo, F. et al. (2015). *JGR, Planets*, *120*, 2020–2035.
[21] Chaffin, M. S., et al.*Nature geoscience* 10.3 (2017): 174-178.
[22] Heavens, Nicholas G., et al.*Nature Astronomy* 2.2 (2018): 126-132.
[23] Vandaele, A. C (2019).*Nature*, *568*(7753), 521-525.
[24] Kahre et al., (this meeting).
[25] Gonzalez- Galindo, et al. (2018). *Journal of Geophysical Research, Planets*, *123*, 1934–1952.
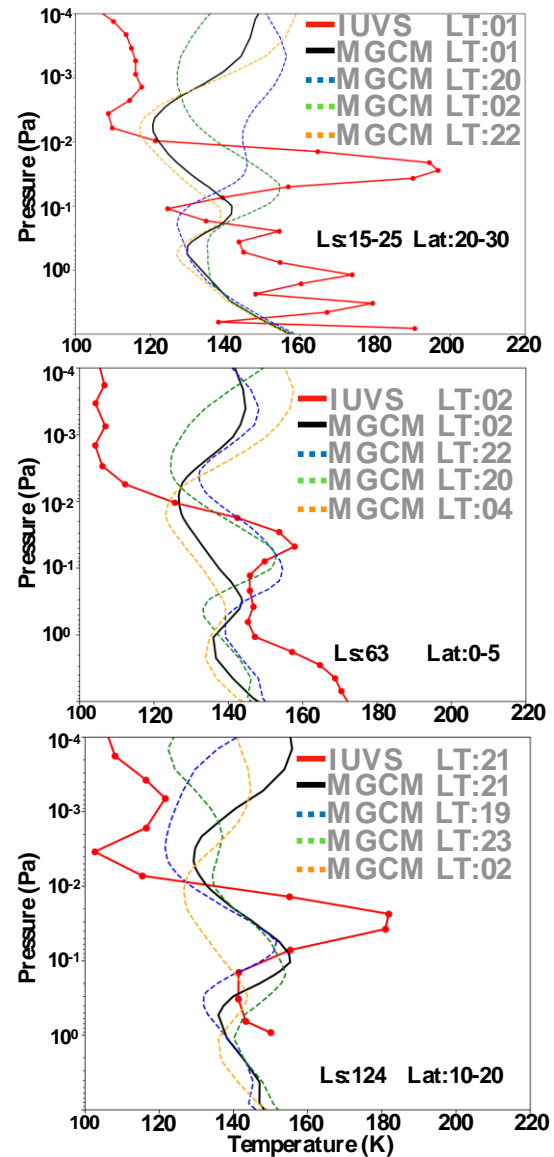
Figure 5: Comparisons with selected verticals profiles that present the recent discovered warm layer, in red solid line and simulations for the same location and time in black solid line. Approximate local time simulations are presented in dashed colored lines to gain better sensation on the time variability of the thermal structure.